

Renat A. Sultanov · D. Guster · S. K. Adhikari

Three-Body Protonium Formation in a Collision Between a Slow Antiproton (\bar{p}) and Muonic Hydrogen: H_μ —Low Energy $\bar{p} + (p\mu^-)_{1s} \rightarrow (\bar{p}p)_{1s} + \mu^-$ Reaction

Received: 25 February 2015 / Accepted: 8 April 2015 / Published online: 1 May 2015
© Springer-Verlag Wien 2015

Abstract A bound state of a proton, p , and its counterpart antiproton, \bar{p} , is a protonium atom $Pn = (\bar{p}p)$. The following three-charge-particle reaction: $\bar{p} + (p\mu^-)_{1s} \rightarrow (\bar{p}p)_{1s} + \mu^-$ is considered in this work, where μ^- is a muon. At low-energies muonic reaction Pn can be formed in the short range state with $\alpha = 1s$ or in the first excited state: $\alpha = 2s/2p$, where \bar{p} and p are placed close enough to each other and the effect of the \bar{p} – p nuclear interaction becomes significantly stronger. The cross sections and rates of the Pn formation reaction are computed in the framework of a few-body approach based on the two-coupled Faddeev-Hahn-type (FH-type) equations. Unlike the original three-body Faddeev method the FH-type equation approach is formulated in terms of only two but relevant components: Ψ_1 and Ψ_2 , of the system's three-body wave function Ψ , where $\Psi = \Psi_1 + \Psi_2$. In order to solve the FH-type equations Ψ_1 is expanded in terms of the input channel target eigenfunctions, i.e. in this work in terms of the $(p\mu^-)$ eigenfunctions. At the same time Ψ_2 is expanded in terms of the output channel two-body wave function, that is in terms of the protonium $(\bar{p}p)$ eigenfunctions. A total angular momentum projection procedure is performed, which leads to an infinite set of one-dimensional coupled integral–differential equations for unknown expansion coefficients.

1 Introduction

Recent progress in the creation of an ultra-slow \bar{p} [1,2] is of considerable scientific interest because of the possible formation of a low-energy anti-hydrogen atom. The main goal of anti-hydrogen/antimatter research is to check and confirm (or not confirm) certain fundamental laws and theories of modern physics. Together with \bar{H} physics, there is a significant interest in the protonium Pn atom too: Pn is a bound state of \bar{p} and p —proton [3]. For example, Pn formation is related to charmonium—a hydrogen-like atom ($\bar{c}c$), which is a bound state of a c -antiquark and c -quark. The \bar{p} – p annihilation can produce ($\bar{c}c$) in the ground and excited states. In this work a few-body system with Coulomb and nuclear forces is considered. Specifically, we compute the cross-sections and rates of an ultra-low energy collision between \bar{p} and a muonic hydrogen atom, i.e. a bound state of p and a negative muon:

$$\bar{p} + (p\mu^-)_{1s} \rightarrow (\bar{p}p)_\alpha + \mu^-. \quad (1)$$

R. A. Sultanov (✉) · D. Guster
Department of Information Systems, BCRL, St. Cloud State University, St. Cloud, MN 56301-4498, USA
E-mail: rasultanov@stcloudstate.edu

R. A. Sultanov · D. Guster
Integrated Science and Engineering Laboratory Facility (ISELF), St. Cloud State University, St. Cloud, MN 56301-4498, USA
E-mail: dcguster@stcloudstate.edu

R. A. Sultanov · S. K. Adhikari
Instituto de Física Teórica, UNESP – Universidade Estadual Paulista, São Paulo, SP 01140, Brazil
E-mail: adhikari@ift.unesp.br

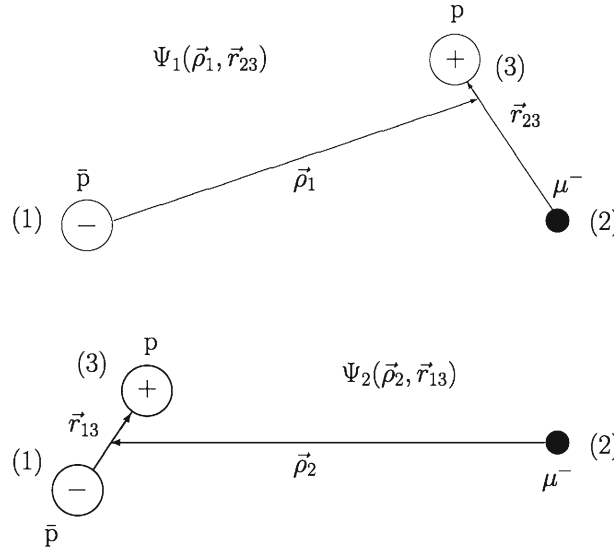


Fig. 1 Two asymptotic spacial configurations of the 3-body system (123), or more specifically (\bar{p}, μ^-, p^+) which is considered in this work. The few-body Jacobi coordinates $(\rho_i, \mathbf{r}_{jk})$, where $i \neq j \neq k = 1, 2, 3$ are also shown together with the 3-body wave function components Ψ_1 and Ψ_2 : $\Psi = \Psi_1 + \Psi_2$ is the total wave function of the 3-body system

Here, $\alpha=1s$, or $2s/2p$ is Pn 's quantum atomic state. At low energies in the muonic reaction (1) protonium can be formed in a very compact, small size ground and "almost" ground states α , in which the hadronic nuclear force between \bar{p} and p should be extremely pronounced. Therefore, it would be interesting to investigate the effect of nuclear forces in this three-body reaction [4]. For example, in the atomic case of the reaction (1), i.e.



Pn would be formed at highly excited "crumbly" states with $\alpha' \approx 30$ [3].

A detailed few-body approach based on a Faddeev-Hahn-type equation formalism is applied in this work [5, 6]. In this approach, the three-body wave function is represented as follows:

$$\Psi = \Psi_1(\mathbf{r}_{23}, \rho_1) + \Psi_2(\mathbf{r}_{13}, \rho_2), \quad (3)$$

where each Faddeev-type component is determined by its own Jacobi coordinates: $\{\mathbf{r}_{ij}, \rho_k\}$ ($i \neq j \neq k = 1, 2, 3$). Furthermore, because we consider the reaction (1) at low energies, i.e. well below the 3-body break-up threshold, the $\Psi_1(\mathbf{r}_{23}, \rho_1)$ component is quadratically integrable over the variable \mathbf{r}_{23} , and the $\Psi_2(\mathbf{r}_{13}, \rho_2)$ component of the total 3-body wave function Ψ is quadratically integrable over the variable \mathbf{r}_{13} in this work. The next section represents the notation pertinent to the three-charge-particle system (123) shown in Fig. 1, the original equations, boundary conditions, detailed derivation of the set of coupled one-dimensional integral–differential equations suitable for a numerical computation and the numerical computational approach developed in this work. The muonic units, i.e. $e = \hbar = m_\mu = 1$, are used in this work, where $m_\mu = 206.769 m_e$ is the mass of the muon.

2 A Few-Body Approach

In this work we consider a Coulomb three-body system with arbitrary masses, i.e. the masses of the charged particles are taken as they are. We do not apply any type of adiabatic approximations, when the dynamics of heavy and light parts of the system are separated. Since the two-body targets are treated equally and the accurate asymptotes for the Ψ_1 and Ψ_2 components are provided, the solution of the FH-type equation avoids the over-completeness problem.

2.1 Basic Equations

Let us define the system of units to be $e = \hbar = m_2 = 1$ and denote antiproton \bar{p} by 1, a negative muon μ^- by 2, and a positive muon μ^+ by 3. Before the three-body breakup threshold two cluster asymptotic configurations are possible in the three-body system, i.e. (23)–1 and (13)–2 being determined by their own Jacobi coordinates $\{\mathbf{r}_{j3}, \boldsymbol{\rho}_k\}$ as shown in Fig. 1:

$$\mathbf{r}_{j3} = \mathbf{r}_3 - \mathbf{r}_j, \quad (4)$$

$$\boldsymbol{\rho}_k = (m_3\mathbf{r}_3 + m_j\mathbf{r}_j)/(m_3 + m_j) - \mathbf{r}_k, \quad (j \neq k = 1, 2). \quad (5)$$

Here \mathbf{r}_ξ , m_ξ are the coordinates and the masses of the particles $\xi = 1, 2, 3$ respectively. This suggests a Faddeev formulation which uses only two components. A general procedure to derive such formulations is described in works [5,6]. In this approach the three-body wave function is represented as follows:

$$|\Psi\rangle = \Psi_1(\mathbf{r}_{23}, \boldsymbol{\rho}_1) + \Psi_2(\mathbf{r}_{13}, \boldsymbol{\rho}_2), \quad (6)$$

where each Faddeev-type component is determined by its own Jacobi coordinates. Moreover, $\Psi_1(\mathbf{r}_{23}, \boldsymbol{\rho}_1)$ is quadratically integrable over the variable \mathbf{r}_{23} , and $\Psi_2(\mathbf{r}_{13}, \boldsymbol{\rho}_2)$ over the variable \mathbf{r}_{13} . To define $|\Psi_l\rangle$, ($l = 1, 2$) a set of two coupled Faddeev-Hahn-type equations can be written [5–7]:

$$(E - \hat{H}_0 - V_{23}(\mathbf{r}_{23}))\Psi_1(\mathbf{r}_{23}, \boldsymbol{\rho}_1) = (V_{23}(\mathbf{r}_{23}) + V_{12}(\mathbf{r}_{12}))\Psi_2(\mathbf{r}_{13}, \boldsymbol{\rho}_2), \quad (7)$$

$$(E - \hat{H}_0 - V_{13}(\mathbf{r}_{13}))\Psi_2(\mathbf{r}_{13}, \boldsymbol{\rho}_2) = (V_{13}(\mathbf{r}_{13}) + V_{12}(\mathbf{r}_{12}))\Psi_1(\mathbf{r}_{23}, \boldsymbol{\rho}_1). \quad (8)$$

Here, \hat{H}_0 is the kinetic energy operator of the three-particle system, $V_{ij}(r_{ij})$ are paired interaction potentials ($i \neq j = 1, 2, 3$), E is the total energy. The constructed equations satisfy the Schrödinger equation exactly. For the energies below the three-body break-up threshold they exhibit the same advantages as the Faddeev equations [8], because they are formulated for the wave function components with the correct physical asymptotes. To solve the equations a close-coupling method is applied, which leads to an expansion of the system's wave function components into eigenfunctions of the subsystem (target) Hamiltonians providing with a set of one-dimensional integral–differential equations after the partial-wave projection. A further advantage of the Faddeev-type method is the fact that the Faddeev-components are smoother functions of the coordinates than the total wave function. Also, the Faddeev decomposition avoids over-completeness problems, because two-body subsystems are treated in an equivalent way, and the correct asymptotes are guaranteed [9,10].

Now, let us present the Eqs. (7)–(8) in terms of the adopted notation:

$$\left(E + \frac{1}{2M_k}\Delta_{\boldsymbol{\rho}_k} + \frac{1}{2\mu_j}\Delta_{\mathbf{r}_{j3}} - V_{j3}\right)\Psi_i(\mathbf{r}_{j3}, \boldsymbol{\rho}_k) = (V_{j3} + V_{jk})\Psi_{i'}(\mathbf{r}_{k3}, \boldsymbol{\rho}_j), \quad (9)$$

here $i \neq i' = 1, 2$, $M_j^{-1} = m_j^{-1} + (m_3 + m_k)^{-1}$, and $\mu_j^{-1} = m_3^{-1} + m_k^{-1}$, where $j \neq k = 1, 2$. In order to separate angular variables, the wave function components Ψ_i are expanded over bipolar harmonics:

$$\{Y_\lambda(\hat{\rho}) \otimes Y_l(\hat{r})\}_{LM} = \sum_{\mu m} C_{\lambda\mu lm}^{LM} Y_{\lambda\mu}(\hat{\rho}) Y_{lm}(\hat{r}), \quad (10)$$

where $\hat{\rho}$ and \hat{r} are angular coordinates of vectors $\boldsymbol{\rho}$ and \mathbf{r} ; $C_{\lambda\mu lm}^{LM}$ are Clebsh–Gordon coefficients; Y_{lm} are spherical functions [11]. Substituting the following expansion:

$$\Psi_i(\mathbf{r}_{j3}, \boldsymbol{\rho}_k) = \sum_{LM\lambda l} \Phi_{LM\lambda l}^i(\rho_k, r_{j3}) \{Y_\lambda(\hat{\rho}_k) \otimes Y_l(\hat{r}_{j3})\}_{LM} \quad (11)$$

into (9), multiplying this by the appropriate biharmonic functions and integrating over the corresponding angular coordinates of the vectors \mathbf{r}_{j3} and $\boldsymbol{\rho}_k$, we obtain a set of equations which for the case of the central potentials has the form:

$$\begin{aligned} & \left(E + \frac{1}{2M_k\rho_k^2} \left\{ \frac{\partial}{\partial \rho_k} \left(\rho_k^2 \frac{\partial}{\partial \rho_k} \right) - \lambda(\lambda+1) \right\} + \frac{1}{2\mu_j r_{j3}^2} \left\{ \frac{\partial}{\partial r_{j3}} \left(r_{j3}^2 \frac{\partial}{\partial r_{j3}} \right) - l(l+1) \right\} - V_{j3}\right) \Phi_{LM\lambda l}^i(\rho_k, r_{j3}) \\ &= \int d\hat{\rho}_k \int d\hat{r}_{j3} \sum_{\lambda' l'} W_{\lambda l \lambda' l'}^{(ii')LM} \Phi_{LM\lambda' l'}^{i'}(\rho_j, r_{k3}), \end{aligned} \quad (12)$$

where the following notation has been introduced:

$$W_{\lambda l \lambda' l'}^{(ii')LM} = \{Y_\lambda(\hat{\rho}_k) \otimes Y_l(\hat{r}_{j3})\}_{LM}^* (V_{j3} + V_{jk}) \{Y_{\lambda'}(\hat{\rho}_j) \otimes Y_{l'}(\hat{r}_{k3})\}_{LM}. \quad (13)$$

To progress from (12) to one-dimensional equations, we apply a modified close coupling method, which consists of expanding each component of the wave function $\Psi_i(\mathbf{r}_{j3}, \boldsymbol{\rho}_k)$ over the Hamiltonian eigenfunctions of subsystems:

$$\hat{h}_{j3} = -\frac{1}{2\mu_j} \nabla_{\mathbf{r}_{j3}}^2 + V_{j3}(\mathbf{r}_{j3}). \quad (14)$$

Thus, following expansions can be applied:

$$\Phi_{LM\lambda l}^i(\rho_k, r_{j3}) = \frac{1}{\rho_k} \sum_n f_{nl\lambda}^{(i)LM}(\rho_k) R_{nl}^{(i)}(r_{j3}), \quad (15)$$

where functions $R_{nl}^{(i)}(r_{j3})$ are defined by the following equation:

$$\left(E_n^i + \frac{1}{2\mu_j r_{j3}^2} \left\{ \frac{\partial}{\partial r_{j3}} \left(r_{j3}^2 \frac{\partial}{\partial r_{j3}} \right) - l(l+1) \right\} - V_{j3} \right) R_{nl}^{(i)}(r_{j3}) = 0. \quad (16)$$

Substituting Eq.(15) into (12), multiplying by the corresponding functions $R_{nl}^{(i)}(r_{j3})$ and integrating over $r_{j3}^2 dr_{j3}$ yields a set of integral–differential equations for the unknown functions $f_{nl\lambda}^{(i)}(\rho_k)$:

$$\begin{aligned} & 2M_k(E - E_n^i) f_{\alpha}^{(i)}(\rho_k) + \left(\frac{\partial^2}{\partial \rho_k^2} - \frac{\lambda(\lambda+1)}{\rho_k^2} \right) f_{\alpha}^{(i)}(\rho_k) \\ &= 2M_k \sum_{\alpha'} \int_0^{\infty} dr_{j3} r_{j3}^2 \int d\hat{r}_{j3} \int d\hat{\rho}_k \frac{\rho_k}{\rho_j} Q_{\alpha\alpha'}^{ii'} f_{\alpha'}^{(i')}(\rho_j), \end{aligned} \quad (17)$$

where

$$Q_{\alpha\alpha'}^{ii'} = R_{nl}^{(i)}(r_{j3}) W_{\lambda l \lambda' l'}^{(ii')LM} R_{n'l'}^{(i')}(r_{k3}). \quad (18)$$

For brevity one can denote $\alpha \equiv nl\lambda$ ($\alpha' \equiv n'l'\lambda'$), and omit LM because all functions have to be the same. The functions $f_{\alpha}^{(i)}(\rho_k)$ depend on the scalar argument, but this set is still not one-dimensional, because formulas are used in different frames of the Jacobi coordinates:

$$\boldsymbol{\rho}_j = \mathbf{r}_{j3} - \beta_k \mathbf{r}_{k3}, \quad (19)$$

$$\mathbf{r}_{j3} = \frac{1}{\gamma} (\beta_k \boldsymbol{\rho}_k + \boldsymbol{\rho}_j), \quad (20)$$

$$\mathbf{r}_{jk} = \frac{1}{\gamma} (\sigma_j \boldsymbol{\rho}_j - \sigma_k \boldsymbol{\rho}_k), \quad (21)$$

with the following mass coefficients:

$$\beta_k = m_k/(m_3 + m_k), \quad \sigma_k = 1 - \beta_k, \quad (22)$$

$$\gamma = 1 - \beta_k \beta_j, \quad (j \neq k = 1, 2), \quad (23)$$

which clearly demonstrates that the modulus of $\boldsymbol{\rho}_j$ depends on two vectors, over which integration on the right-hand sides is accomplished. It follows from Eq.(20), that: $\boldsymbol{\rho}_j = \gamma \mathbf{r}_{j3} - \beta_k \boldsymbol{\rho}_k$. Therefore, to obtain one-dimensional integral–differential equations, corresponding to Eq.(17), we will proceed with the integration over variables $\{\boldsymbol{\rho}_j, \hat{\rho}_k\}$, rather than $\{\mathbf{r}_{j3}, \hat{\rho}_k\}$. The Jacobian of this transformation is $J = \gamma^{-3}$. Thus, we arrive at a set of one-dimensional integral–differential equations:

$$2M_k(E - E_n^i) f_{\alpha}^{(i)}(\rho_k) + \left(\frac{\partial^2}{\partial \rho_k^2} - \frac{\lambda(\lambda+1)}{\rho_k^2} \right) f_{\alpha}^{(i)}(\rho_k) = \frac{M_k}{\gamma^{-3}} \sum_{\alpha'} \int_0^{\infty} d\rho_j S_{\alpha\alpha'}^{ii'}(\rho_j, \rho_k) f_{\alpha'}^{(i')}(\rho_j), \quad (24)$$

where functions $S_{\alpha\alpha'}^{ii'}(\rho_j, \rho_k)$ are defined as follows:

$$S_{\alpha\alpha'}^{ii'}(\rho_j, \rho_k) = 2\rho_j\rho_k \int d\hat{\rho}_j \int d\hat{\rho}_k R_{nl}^{(i)}(r_{j3}) \{Y_\lambda(\hat{\rho}_k) \otimes Y_l(\hat{r}_{j3})\}_{LM}^* (V_{j3} + V_{jk}) \\ \times \{Y_{\lambda'}(\hat{\rho}_j) \otimes Y_{l'}(\hat{r}_{k3})\}_{LM} R_{n'l'}^{(i')}(r_{k3}). \quad (25)$$

One can show [9, 10] that fourfold multiple integration in Eq. (25) leads to a one-dimensional integral and the expression (25) could be determined for any orbital momentum value L :

$$S_{\alpha\alpha'}^{ii'}(\rho_j, \rho_k) = \frac{4\pi}{2L+1} [(2\lambda+1)(2\lambda'+1)]^{\frac{1}{2}} \rho_j\rho_k \int_0^\pi d\omega \sin \omega R_{nl}^{(i)}(r_{j3}) (V_{j3}(r_{j3}) + V_{jk}(r_{jk})) \\ \times R_{n'l'}^{(i')}(r_{k3}) \sum_{mm'} D_{mm'}^L(0, \omega, 0) C_{\lambda 0 l m}^{Lm} C_{\lambda' 0 l' m'}^{Lm'} Y_{lm}(v_j, \pi) Y_{l'm'}^*(v_k, \pi), \quad (26)$$

where $D_{mm'}^L(0, \omega, 0)$ are Wigner functions, ω is the angle between ρ_j and ρ_k , v_j is the angle between \mathbf{r}_{k3} and ρ_j , v_k is the angle between \mathbf{r}_{j3} and ρ_k .

Finally, we obtain an infinite set of one-dimensional coupled integral–differential equations for the unknown functions $f_\alpha^1(\rho_1)$ and $f_{\alpha'}^2(\rho_2)$ [9, 10]:

$$\left[(k_n^i)^2 + \frac{\partial^2}{\partial \rho_i^2} - \frac{\lambda(\lambda+1)}{\rho_i^2} \right] f_\alpha^{(i)}(\rho_i) = g_i \sum_{\alpha'} \sqrt{\frac{(2\lambda+1)(2\lambda'+1)}{(2L+1)^2}} \int_0^\pi d\rho_{i'} f_{\alpha'}^{(i')}(\rho_{i'}) \\ \times \int_0^\pi d\omega \sin \omega R_{nl}^{(i)}(r_{i'3}) (V_{i'3}(r_{i'3}) + V_{ii'}(r_{ii'})) R_{n'l'}^{(i')}(r_{i3}) \rho_{i'} \rho_i \\ \times \sum_{mm'} D_{mm'}^L(0, \omega, 0) C_{\lambda 0 l m}^{Lm} C_{\lambda' 0 l' m'}^{Lm'} Y_{lm}(v_i, \pi) Y_{l'm'}^*(v_{i'}, \pi). \quad (27)$$

For the sake of simplicity $\alpha \equiv (nl\lambda)$ are quantum numbers of a three-body state and L is the total angular momentum of the three-body system, $i \neq i' = 1, 2$, $g_i = 4\pi M_i/\gamma^3$, $k_n^i = \sqrt{2M_i(E - E_n^{i'})}$, where $E_n^{i'}$ is the binding energy of the subsystem ($i'3$), $M_1 = m_1(m_2 + m_3)/(m_1 + m_2 + m_3)$ and $M_2 = m_2(m_1 + m_3)/(m_1 + m_2 + m_3)$ are the reduced masses, $\gamma = 1 - m_i m_{i'}/((m_i + m_3)(m_{i'} + m_3))$, $D_{mm'}^L(0, \omega, 0)$ the Wigner functions, $C_{\lambda 0 l m}^{Lm}$ the Clebsh–Gordon coefficients, Y_{lm} are the spherical functions, ω is the angle between the Jacobi coordinates ρ_i and $\rho_{i'}$, v_i is the angle between $\mathbf{r}_{i'3}$ and ρ_i , $v_{i'}$ is the angle between \mathbf{r}_{i3} and $\rho_{i'}$. One can show that: $\sin v_i = \rho_{i'}/(\gamma r_{i'3}) \sin \omega$ and $\cos v_i = (\beta_i \rho_i + \rho_{i'} \cos \omega)/(\gamma r_{i'3})$.

2.2 K -Matrix Approach and Numerical Implementation

To find a unique solution to Eq. (27) appropriate boundary conditions, depending on the specific physical situation, need to be considered. First we impose:

$$f_{nl}^{(i)}(0) \sim 0. \quad (28)$$

Next, for the three-body charge-transfer problem we apply the well known \mathbf{K} –matrix formalism. This method has already been applied for solution of three-body problems in the framework of the coordinate space Faddeev equations. For the present scattering problem with $i + (j3)$ as the initial state, in the asymptotic region, it takes two solutions to Eq. (27) to satisfy the following boundary conditions:

$$\begin{cases} f_{1s}^{(i)}(\rho_i) \underset{\rho_i \rightarrow +\infty}{\sim} \sin(k_{n=1}^{(i)} \rho_i) + K_{ii} \cos(k_{n=1}^{(i)} \rho_i) \\ f_{1s}^{(j)}(\rho_j) \underset{\rho_j \rightarrow +\infty}{\sim} \sqrt{v_i/v_j} K_{ij} \cos(k_{n=1}^{(j)} \rho_j) \end{cases} \quad (29)$$

where ($i \neq j=1, 2$), K_{ij} are the appropriate coefficients, and v_i is a velocity in channel i . With the following change of the variables in the Eq. (27):

$$f_{1s}^{(i)}(\rho_i) = f_{1s}^{(i)}(\rho_i) - \sin(k_{n=1}^{(i)}\rho_i), \quad (30)$$

we get two sets of inhomogeneous equations which are solved numerically. The coefficients K_{ij} can be obtained from a numerical solution of the FH-type equations. The cross sections are given by the following expression:

$$\sigma_{ij} = \frac{4\pi}{k_{n=1}^{(i)2}} \left| \frac{\mathbf{K}}{1 - \mathbf{i}\mathbf{K}} \right|^2 = \frac{4\pi}{k_{n=1}^{(i)2}} \frac{\delta_{ij} D^2 + K_{ij}^2}{(D - 1)^2 + (K_{11} + K_{22})^2}, \quad (31)$$

where ($i, j = 1, 2$) refer to the two channels, $D = K_{11}K_{22} - K_{12}K_{21}$ and bold \mathbf{i} is the imaginary unit. Also, from the quantum-mechanical unitarity principle one can derive that the scattering matrix:

$$\mathbf{K} = \begin{pmatrix} K_{11} & K_{12} \\ K_{21} & K_{22} \end{pmatrix} \quad (32)$$

has the following important feature $K_{12} = K_{21}$, that is:

$$\chi(E) = K_{12}/K_{21} = 1.0, \quad (33)$$

which is automatically checked in our FORTRAN code at any collision energy between \bar{p} and H_μ .

To solve the coupled integral–differential equations (27) one needs to first compute the angular integrals Eq. (26). They are independent of energy E . Therefore, one needs to compute them only once and then store them on a computer's hard drive (or solid state drive) to support future computation of other observables, i.e. the charge-transfer cross-sections at different collision energies. The sub-integral expressions in (26) have a very strong and complicated dependence on the Jacobi coordinates ρ_i and $\rho_{i'}$. To calculate $S_{\alpha\alpha'}^{(ii')}(\rho_i, \rho_{i'})$ at different values of ρ_i and $\rho_{i'}$ an adaptable algorithm has been applied together with the following mathematical substitution: $\cos \omega = (x^2 - \beta_i^2 \rho_i^2 - \rho_{i'}^2)/(2\beta_i \rho_i \rho_{i'})$. The angle dependent part of the equation can be written as the following one-dimensional integral:

$$S_{\alpha\alpha'}^{(ii')}(\rho_i, \rho_{i'}) = \frac{4\pi}{\beta_i} \frac{[(2\lambda + 1)(2\lambda' + 1)]^{\frac{1}{2}}}{2L + 1} \int_{|\beta_i \rho_i - \rho_{i'}|}^{\beta_i \rho_i + \rho_{i'}} dx R_{nl}^{(i)}(x) \left[-1 + \frac{x}{r_{ii'}(x)} \right] R_{n'l'}^{(i')}(r_{i3}(x)) \times \sum_{mm'} D_{mm'}^L(0, \omega(x), 0) C_{\lambda 0 l m}^{Lm} C_{\lambda' 0 l' m'}^{Lm'} Y_{lm}(v_i(x), \pi) Y_{l'm'}^*(v_{i'}(x), \pi). \quad (34)$$

We used a special adaptive FORTRAN subroutine in order to carry out the angle integration in (34). The set of truncated integral–differential Eq. (27) is solved by a discretization procedure, i.e. on the right side of the equations the integrals over ρ_1 and ρ_2 are replaced by sums using the trapezoidal rule and the second order partial derivatives on the left side are discretized using a three-point rule. By this means we obtain a set of linear equations for the unknown coefficients $f_\alpha^{(i)}(k)$ ($k = 1, N_p$):

$$\left[k_n^{(1)2} + D_{ij}^2 - \frac{\lambda(\lambda + 1)}{\rho_{1i}^2} \right] f_\alpha^{(1)}(i) - \frac{M_1}{\gamma^3} \sum_{\alpha'=1}^{N_s} \sum_{j=1}^{N_p} w_j S_{\alpha\alpha'}^{(12)}(\rho_{1i}, \rho_{2j}) f_{\alpha'}^{(2)}(j) = 0, \quad (35)$$

$$- \frac{M_2}{\gamma^3} \sum_{\alpha=1}^{N_s} \sum_{j=1}^{N_p} w_j S_{\alpha\alpha}^{(21)}(\rho_{2i}, \rho_{1j}) f_\alpha^{(1)}(j) + \left[k_{n'}^{(2)2} + D_{ij}^2 - \frac{\lambda'(\lambda' + 1)}{\rho_{2i}^2} \right] f_{\alpha'}^{(2)}(i) = B_{\alpha'}^{21}(i). \quad (36)$$

Here, coefficients w_j are weights of the integration points ρ_{1i} and ρ_{2i} ($i = 1, N_p$), N_s is the number of quantum states which are taken into account in the expansion (15). Next, D_{ij}^2 is the three-point numerical approximation for the second order differential operator: $D_{ij}^2 f_\alpha(i) = (f_\alpha(i-1)\delta_{i-1,j} - 2f_\alpha(i)\delta_{i,j} + f_\alpha(i+1)\delta_{i+1,j})/\Delta$, where Δ is a step of the grid $\Delta = \rho_{i+1} - \rho_i$. The vector $B_{\alpha'}^{21}(i)$ is: $B_{\alpha'}^{(21)}(i) =$

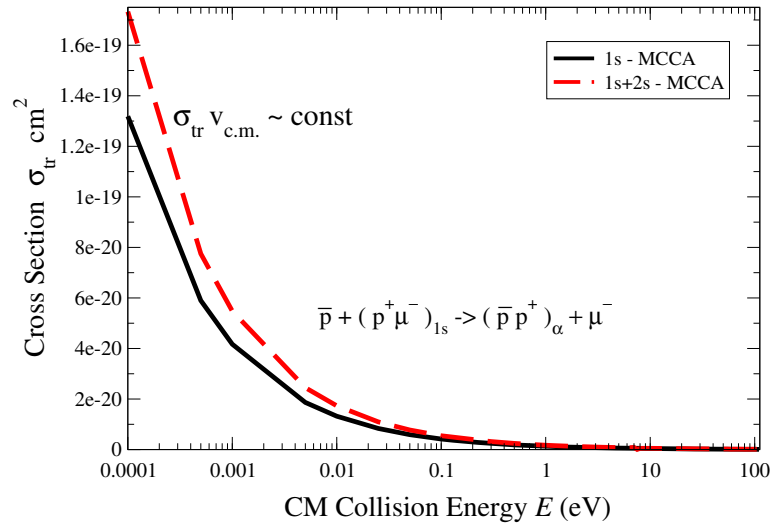


Fig. 2 This figure shows our numerical result for the low-energy proton transfer reaction integral cross section σ_{tr} in the three-charge-particle collision $\bar{p} + H_\mu \rightarrow (\bar{p}p)_\alpha + \mu^-$, where H_μ is a muonic hydrogen atom: a bound state of a proton and a negative muon. In this work only the reaction channel with $\alpha=1s$ is considered in the framework of the $1s$ and $1s + 2s$ modified close-coupling approximation (MCCA) approach

$M_2/\gamma^3 \sum_{j=1}^{N_p} w_j S_{\alpha'1s0}^{(21)}(i, j) \sin(k_{n=1}^{(j)} \rho_j)$, and in symbolic-operator notations the set of linear Eqs. (35)–(36) has the following form:

$$\sum_{\alpha'=1}^{2 \times N_s} \sum_{j=1}^{N_p} \mathbf{A}_{\alpha\alpha'}(i, j) \mathbf{f}_{\alpha'}(j) = \mathbf{b}_\alpha(i). \quad (37)$$

The discretized equations are subsequently solved by the Gauss elimination method. As can be seen from Eqs. (35)–(36) the matrix \mathbf{A} should have a so-called block-structure: there are four main blocks in the matrix: two of them related to the differential operators and other two to the integral operators. Each of these blocks should have sub-blocks depending on the quantum numbers $\alpha = n l \lambda$ and $\alpha' = n' l' \lambda'$. The second order differential operators produce three-diagonal sub-matrices.

3 Results

In this section we report our *preliminary* computational results. We compare some of our new findings with the corresponding data from older work [12]. The Pn formation cross section in the reaction (1) are shown in Fig. 2. Here we used only $1s$ and $1s + 2s$ states within the modified close-coupling approximation (MCCA) approach. One can see that the contribution of the $2s$ -states from each target is becoming even more significant while the collision energy becomes smaller. Additionally, for the process (1) we compute the numerical value of the following important quantity: $\Lambda(Pn) = \sigma_{tr}(E \rightarrow 0) v_{c.m.} \approx \text{const}$, which is proportional to the actual Pn formation rate at low collision energies. Table 1 includes our data for this important parameter together with the Pn formation total cross section. All these results are obtained in the framework of the $2 \times (1s)$ and $2 \times (1s + 2s)$ approximations. The sign " $2 \times$ " means that two sets of the expansion functions from each target are applied. Therefore, for example, in the case of the $1s$ MCCA approach two expansion functions are used in our calculations. However, in the case of the $1s + 2s$ MCCA approach four expansion functions are applied. Additionally, as we mentioned above, the unitarity relationship, i.e. Eq. (33), is checked for all considered collision energies E . It is seen, that $\chi(E)$ possesses a fairly constant value close to one. Now, in the framework of the $2 \times (1s + 2s + 2p)$ MCCA approach, i.e. when six coupled Faddeev-Hahn-type integral-differential equations are solved, our result for the Pn formation rate has the following value: $\Lambda_{1s2s2p}^{Pn} = \sigma_{tr} \times v_{c.m.} \approx 0.27$ m.a.u. The corresponding rate from the work [12] is: $\Lambda'(Pn) \approx 0.2$ m.a.u. Both results are in a fairly good agreement with each other and were multiplied by 5 as in [12]. In conclusion, because of the complexity of the few-body system and the method, in this work only the total orbital momentum $L = 0$ has been taken into account. It was adequate in the case of the slow and ultraslow collisions discussed above. Also, we understand

Table 1 The total Pn formation cross section σ_{tr} in the three-body reaction (1), when $\alpha = 1$, and a product of this cross section and the corresponding center-of-mass velocities $v_{c.m.}$ between \bar{p} and H_μ .

E , eV	$2 \times (1s)$ —MCCA approach		$2 \times (1s + 2s)$ —MCC approach		
	σ_{tr} , cm ²	$\sigma_{tr} \times v_{c.m.}$, m.a.u	σ_{tr} , cm ²	$\sigma_{tr} \times v_{c.m.}$, m.a.u	$\chi(E)$, Eq.(33)
0.0001	0.1319E-18	0.8776E-01	0.1733E-18	0.1153	0.9976
0.0005	0.5897E-19	0.8776E-01	0.7749E-19	0.1153	0.9976
0.0010	0.4170E-19	0.8776E-01	0.5479E-19	0.1153	0.9976
0.0050	0.1865E-19	0.8776E-01	0.2450E-19	0.1153	0.9976
0.0100	0.1319E-19	0.8775E-01	0.1733E-19	0.1153	0.9976
0.0500	0.5895E-20	0.8773E-01	0.7748E-20	0.1153	0.9977
0.1000	0.4168E-20	0.8771E-01	0.5478E-20	0.1153	0.9977
0.5000	0.1860E-20	0.8753E-01	0.2450E-20	0.1153	0.9982
1.0000	0.1312E-20	0.8731E-01	0.1733E-20	0.1153	0.9988
2.0000	0.9228E-21	0.8685E-01	0.1227E-20	0.1155	1.0002
4.0000	0.6441E-21	0.8574E-01	0.8767E-21	0.1167	1.0002
7.0000	0.4404E-21	0.7754E-01	0.8728E-21	0.1537	1.0006

The results are presented together with the corresponding unitarity ratio between the K_{12} and K_{21} coefficients of the scattering K -matrix, Eq.(32). These results are provided in the $2 \times (1s)$ and $2 \times (1s + 2s)$ modified close coupling approximation (MCCA) approach

that it would be useful to take into account higher atomic target states like $3s + 3p + 3d + 4s + \dots$ as well as the continuum spectrum. This calculation would be an interesting future work. However, at very low energy collisions, which are considered in this paper, all these channels are closed and located far away from the actual collision energies. At the same time the main contribution from s- and p-states (polarization) is taken into account.

A direct inclusion of the strong \bar{p} -p interaction [4] would be a very interesting future investigation in the framework of the three-body reaction (1).

Acknowledgments This work was supported by the Office of Research and Sponsored Programs of St. Cloud State University, USA and CNPq and FAPESP of Brazil.

References

1. Gabrielse, G. (ATRAP Collaboration) et al.: Adiabatic cooling of antiprotons. Phys. Rev. Lett. **106** 073002 (2011)
2. Andresen, G. B. (ALPHA Collaboration) et al.: Evaporative cooling of antiprotons to cryogenic temperatures. Phys. Rev. Lett. **105** 013003 (2010)
3. Sakimoto, K.: Unified treatment of hadronic annihilation and protonium formation in slow collisions of antiprotons with hydrogen atoms. Phys. Rev. A **88**, 012507 (2013)
4. Richard, J.M., Sainio, M.E.: Nuclear effects in protonium. Phys. Lett. B **110**, 349–352 (1982)
5. Hahn, Y., Watson, K.M.: Reduction method and distortion potentials for many-particle scattering equations. Phys. Rev. A **5**, 1718–1725 (1972)
6. Hahn, Y.: Reduced matrix equations with reactive components for direct nuclear interactions. Nucl. Phys. A **389**, 1–17 (1982)
7. Sultanov, R.A., Adhikari, S.K.: Coordinate-space Faddeev-Hahn-type approach to three-body charge-transfer reactions involving exotic particles. Phys. Rev. A **61**, 227111 (2000)
8. Faddeev, L.D.: Mathematical Aspects of the Three-Body Problem in the Quantum Scattering Theory. Israel Program for Scientific Translation, Jerusalem (1965)
9. Sultanov, R.A., Guster, D.: Antihydrogen (\bar{H}) and muonic antihydrogen (\bar{H}_μ) formation in low energy three-charge-particle collisions. J. Phys. B At. Mol. Opt. Phys. **46**, 215204 (2013)
10. Sultanov, R.A., Guster, D.: Antiproton low-energy collisions with Ps-atoms and true muonium atoms ($\mu^+\mu^-$): \bar{H} and \bar{H}_μ three-body formation reactions. Hyperfine Interact. **228**, 47–52 (2014)
11. Varshalovich, D.A., Moskalev, A.N., Khersonskii, V.L.: Quantum Theory of Angular Momentum. World Scientific, Singapore (1988)
12. Igarashi, A., Toshima, N.: Application of hyperspherical close-coupling method to antiproton collisions with muonic hydrogen. Eur. Phys. J. D **46**, 425–430 (2008)